Improving Small Cell Capacity with Common-Carrier Full Duplex Radios

Sanjay Goyal, Pei Liu, Shivendra Panwar
Polytechnic Institute of New York University
Brooklyn, NY, USA
sgoyal01@students.poly.edu, pliu@poly.edu,
panwar@catt.poly.edu

Robert A. DiFazio, Rui Yang, Jialing Li, Erdem Bala
InterDigital Communications, Inc.
Melville, NY, USA
{robert.difazio, rui.yang, jialing.li, erdem.bala}
@interdigital.com

***Abstract*— Recent progress in establishing the capability of radios to operate in full duplex mode on a single channel has been attracting growing attention from many researchers. We extend this work by considering the application to small cells, in particular resource-managed cellular systems similar to the TDD variant of LTE. We derive conditions where full duplex operation provides improved throughput compared to half duplex for a single cell scenario. We present a hybrid scheduler that defaults to half duplex operation but can assign full duplex timeslots when it is advantageous to do so. We compare the performance of such a scheduler with a traditional half duplex scheduler in terms of throughput and energy efficiency. Our simulation results show that we achieve as much as 81% of the capacity doubling promised by full duplex, with limitations deriving from interference effects specific to full duplex operation.**

I. Introduction

The demand for wireless data increases year after year driven by the growth of smart phones, tablets, laptops sales, the popularity of video streaming, and other bandwidth intensive applications. Regulatory bodies and companies have highlighted this trend with various estimates of spectrum shortage and have proposed ways forward [1]–[4]. There have even been goals set to improve capacity by as much as 1000x [5], [6]. Meeting the demand, simple in concept but often challenging in implementation, falls into two categories: more spectrum or more efficient use of current spectrum. The latter includes radio link design such as waveforms and channel coding enhancements; network architecture evolution towards small cells, heterogeneous networks, and multi-cell cooperation; and improvements in source coding and video compression. This paper addresses a promising radio link approach, the use of full duplex operation in a single RF channel that has the potential to double the spectral efficiency.

The large differential between transmitted (Tx) and received (Rx) powers in an RF link, together with typical Tx/Rx isolation, has driven the vast majority of systems to either frequency division duplexing (FDD) or time division duplexing (TDD). FDD separates the Tx and Rx signals with filters and TDD with Tx/Rx switching. Recent results have challenged this limitation and established the feasibility of full duplex common carrier operation by demonstrating that a combination of analog cancellation and digital cancellation can remove enough of the Tx self-interference from the Rx path to allow demodulation of the received signal. This was demonstrated using multiple antennas positioned for optimum cancellation in [7] and later as single antenna systems [8], [9] where as much as 110 dB cancellation is reported, compared to more typical results of 85 dB. An antenna feed network, for which a prototype provided 40 to 45 dB Tx/Rx isolation before analog and digital cancellation, was described in [8]. An 802.11 system, with the CSMA/CA MAC slightly modified for full duplex operation, is presented in [10], [11], and [12] where software simulations show throughput gains from 1.2 to 2.0 assuming 85 dB cancellation. A multi macro cell network with full duplex base stations is analyzed in [13], where an analytical model based on stochastic geometry shows the throughput gain of 11% and 91% in uplink and downlink, respectively, due to full duplex BSs deployment. They also derived the full duplex gain through simulating an OFDMA based system, where it shows the throughput gain of 57% and 99% in uplink and downlink, respectively. Uplink gain is limited by the high inter cell interference from the neighboring BSs during full duplex operation. In their design they did not include the effect of residual self-interference at BSs, which may restrict one from using the full duplex technology in a large cell scenario because of the lower uplink coverage due to self-interference effect. A performance comparison in terms of capacity enhancement between using multiple-antennas as half duplex MIMO with that of utilizing them to build a full duplex radio in a single cell scenario is done in [14]. They used the information theoretic techniques, that is, successive interference cancellation for uplink and dirty paper coding in downlink to calculate the user capacity. It shows that under certain conditions, using additional antennas for building full-duplex radio can provide performance boost compared to utilizing them to form a high capacity MIMO link.

Our work accepts the premise that transceivers with sufficient cancellation technology are feasible, and focuses on the application of full duplex common carrier operation in resource managed TDMA-type small cell systems with dynamic scheduling. A current example is LTE, in particular, the TDD variant [15], [16]. Providing a factor of two times increase in capacity would be a significant breakthrough, yet

This work is partially supported by NSF's Accelerating Innovation Research Project.

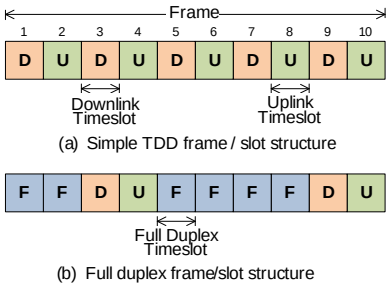

Fig. 1: TDD half duplex baseline and full duplex operation.

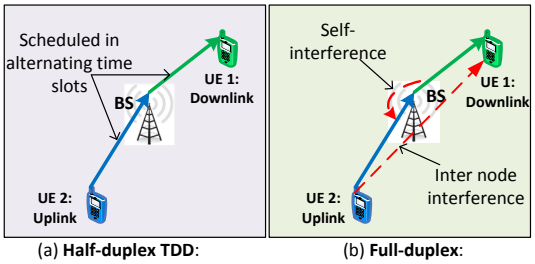

(a) **Half-duplex TDD**: UE 1 and UE 2 are scheduled on alternating time slots

(b) **Full-duplex**: UE 1 and UE 2 are scheduled at the same time slot on the same channel

Fig. 2: Half duplex and full duplex single cell scenarios.

given the variety of link geometries, the density of users, and propagation effects in mobile channels, the problem we address is to determine what level of capacity improvement can indeed be expected. We begin with a single small cell, using propagation models proposed by 3GPP for the evaluation of small cell hot zones [17]. The base stations are assumed to be capable of full duplex operation, where the additional cost and power is most likely to be acceptable, while the mobile stations are limited to half duplex operation. We evaluate link conditions under which full duplex operation can be supported, present scheduling approaches for both a half duplex baseline and full duplex operation, compare the throughput of the systems, and evaluate energy efficiency.

Section II presents the communication system scenario. Conditions for full duplex operation, including range and self-interference cancellation, are derived in Section III. Scheduling algorithms for half duplex and full duplex operation are provided in Section IV. Section V contains simulation results for throughput and energy efficiency. Conclusions are discussed in Section VI.

II. A Full Duplex Single Small Cell

We consider a scenario consisting of a small cell with multiple legacy half duplex user equipment (UEs) and a base station (BS) that can operate in full duplex or half duplex mode. Figure 1(a) shows the half duplex TDD baseline. It consists of a frame containing a set of timeslots, all operating on the same frequency channel, that alternate between uplink and downlink operation providing a continuous stream of data in one direction or the other. This is a simplified structure in that a deployed system, TDD LTE for example [15], [16], would typically have special timeslots or guard periods for Tx/Rx switching and other overhead functions and may group uplink and downlink slots together to minimize switching, which we do not consider in our current analysis. Full duplex timeslots are introduced in Figure 1(b). It would be desirable to configure every timeslot as full duplex in the hope of achieving a doubling of capacity, but we anticipate the need to operate some as either solely uplink or solely downlink due to the interference environment explained below. It is the job of a packet scheduler to determine whether a timeslot will be an uplink, downlink, or full duplex timeslot and which UE will be given service.

The half duplex TDD scenario is further illustrated in Figure 2(a) where UE1 is a downlink user and UE2 is an uplink user. The orthogonal channel access in time, as shown in Figure 1(a), prevents interference between UEs, but each UE only accesses the channel half the time. Figure 2(b) shows the full duplex scenario where both UEs are scheduled in the same timeslot, potentially doubling the total cell throughput. Unfortunately, there are several interference issues that need to be considered: (1) the Tx-to-Rx self-interference at the BS which impacts the ability of the BS to demodulate the uplink signal, and (2) the interference from UE2's uplink signal which impacts the ability of UE1 to demodulate its downlink signal. Depending on the locations of the two UEs relative to each other and the BS, the propagation channels, the self interference cancellation capability of the BS, the required SNR at each receiver, and the limit of Tx power, the use of full duplex operation may lead to lower throughput compared to half duplex operation. So, a doubling of capacity is only an upper bound, and the actual full duplex gain needs to be evaluated which is the subject of the remainder of this paper.

III. Conditions for Full Duplex Gain in a Single Small Cell

In this section, we derive the conditions, one for downlink and the other for uplink, under which full duplex operation will have throughput gain in comparison to the baseline half duplex TDD system. We use the capacity upper bound as the metric to measure such gain. The expressions of the conditions illustrate the dependencies among various system parameters mentioned in the previous section. More importantly, the existence of common parameters in those conditions implies that downlink-uplink joint optimization is desirable to maximize the system sum capacity.

A. Condition for full duplex gain in downlink

In the full duplex system, a downlink UE gets twice as many timeslots, albeit subject to interference from an uplink UE on the same channel. Therefore, full duplex operation will provide a net throughput gain on the downlink when the downlink data transfer across two timeslots, subject to interference from the uplink UE, is larger than the downlink throughput in one timeslot without any such interference (i.e., the half duplex baseline).

Consider Figure 3 where a downlink user UE1 is at distance d_1 meters away from its BS, which is transmitting at power P_{BS} watts. The channel between UE1 and the BS is given

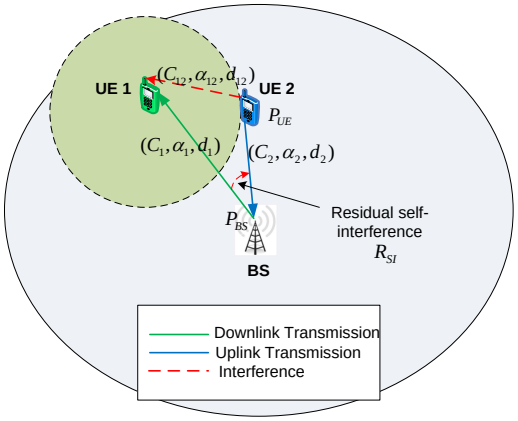

Fig. 3: A full-duplex small cell showing the interference range.

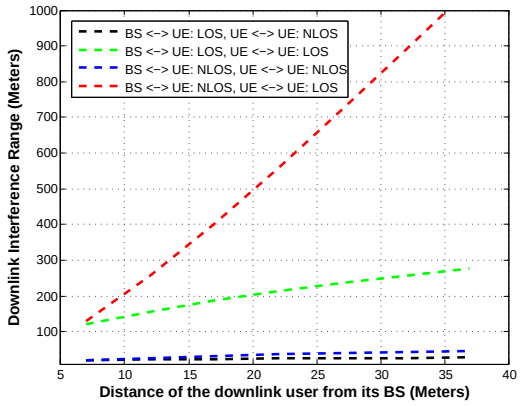

Fig. 4: Downlink interference range with different channel conditions (P_{BS} = 1.78 dBm, and P_{UE} = 0.78 dBm).

by $(a_1 d_1^{\alpha_1/2})^{-1}$ where α_1 is the path loss exponent, and $C_1 = |a_1|^2$ includes shadowing and the constant factor in the path loss. The uplink user UE2 on the same channel is transmitting at power P_{UE} watts. It is at d_{12} meters away from the UE1, and the channel between UE1 and UE2 is given by $(a_{12} d_{12}^{\alpha_{12}/2})^{-1}$, for which we use $C_{12} = |a_{12}|^2$ in below equations.

Assuming half duplex system, the downlink user UE1's data rate is

$$R_{HD} = W_C \ log_2(1 + SNR_{HD}), \tag{1}$$

where

$$SNR_{HD} = \frac{P_{BS}}{C_1 d_1^{\alpha_1}} \ \frac{1}{N_{UE}}. \tag{2}$$

In the above equations, W_C is the bandwidth of a channel which is shared for the uplink and downlink transmission and N_{UE} is the noise power at the UE1. In a full duplex system, where the downlink UE is also scheduled in the uplink time interval and the channel stays constant in both intervals, UE1 gets the data rate

$$R_{FD} = 2W_C \ log_2(1 + SINR_{FD}), \tag{3}$$

where

$$SINR_{FD} = \frac{P_{BS}}{C_1 d_1^{\alpha_1}} \ \frac{1}{(N_{UE} + I_{UE})}, \tag{4}$$

where I_{UE} is the interference power from the uplink user (UE2), which is given by

$$I_{UE} = \frac{P_{UE}}{C_{12} d_{12}^{\alpha_{12}}}. \tag{5}$$

To achieve full duplex gain, the data rates for full duplex and half duplex systems need to satisfy the following condition:

$$R_{FD} > R_{HD} \tag{6}$$

Using expressions in (1)-(5), the above inequality can be expressed as

$$\left(\frac{P_{UE}}{C_{12} d_{12}^{\alpha_{12}}}\right)^2 - N_{UE}\left(N_{UE} + \frac{P_{BS}}{C_1 d_1^{\alpha_1}}\right) < 0 \tag{7}$$

This is the condition for full duplex gain in downlink. Given channel characteristics and received noise power at UE1, this condition is a function of UE2 and BS transmit powers (i.e., P_{UE}, and P_{BS}), and the distances between the two UEs (d_{12}) and between the BS and UE1 (d_1).

The condition expressed in (7) can be used for different purposes. For example, given the location of the UEs, it can be used to set power levels to achieve high throughput using full duplex operation. If transmit powers are fixed, it could also be used to determine if it would be better to use full duplex or half duplex operation depending on the distance between two UEs. In fact, from (7), one can get

$$d_{12} > \left(\frac{P_{UE}}{C_{12}}\left(\frac{P_{BS} N_{UE}}{C_1 d_1^{\alpha_1}} + {N_{UE}}^2\right)^{-1/2}\right)^{1/\alpha_{12}} \tag{8}$$

The expression on the right hand side of the above expression is the minimum required distance between an uplink UE and a downlink UE to achieve full duplex downlink gain. Figure 4 shows the results for various channel conditions as a function of the distance between the downlink UE and the base station. In the figure, BS↔UE:LOS and UE↔UE:NLOS mean that the channel between the downlink UE and the BS has line-of-sight (LOS) propagation (α_1=1.69), and the channel between UEs (interfering uplink UE and the downlink UE) has non-line-of-sight (NLOS) propagation (α_{12}=4.33), respectively. The BS power (P_{BS}) and UE power (P_{UE}) are set to 1.78 dBm and 0.78 dBm, respectively. (Further details of the simulation parameters are given in Section V.) Not surprisingly, the results in Figure 4 indicate that the downlink propagation channel from the BS to UE1 must be favorable, or at least comparable to the interference channel from UE2 to UE1 for full duplex operation to be feasible.

B. Condition for full duplex gain in uplink

As shown in Figure 3, an uplink user UE2, which is at d_2 meters away from the BS, is transmitting at P_{UE} on an uplink channel given by $(a_2 d_2^{\alpha_2/2})^{-1}$, for which we use $C_2 = |a_2|^2$ in below equations. During full duplex operation, the BS schedules a downlink user UE1 on the same channel. It transmits at P_{BS} which causes self interference power of R_{SI} to the uplink receiver.

Similar to Section III-A, the data rate of the uplink UE in the half duplex and the full duplex systems are given by (1), and (3), respectively. In the uplink case,

$$SNR_{HD} = \frac{P_{UE}}{C_2 d_2^{\alpha_2}} \ \frac{1}{N_{BS}}, \tag{9}$$

and

$$SINR_{FD} = \frac{P_{UE}}{C_2 d_2^{\alpha_2}} \ \frac{1}{(N_{BS} + R_{SI})}, \tag{10}$$

where N_{BS} is the noise power at the BS. In this paper, we consider a basic self-interference model in which the cancellation capability does not vary with the transmission power, so for the given transmission power P_{BS} and the self-interference cancellation value C_{SI}, the residual self-interference power is given by

$$R_{SI} = \frac{P_{BS}}{C_{SI}}. \tag{11}$$

To achieve full duplex gain, the data rates for full duplex and half duplex systems need to satisfy the following condition:

$$R_{FD} > R_{HD} \tag{12}$$

Using expressions in (9)-(11), the above inequality can be expressed as

$$\left(\frac{P_{UE}}{C_2 d_2^{\alpha_2}}\right) N_{BS} + N_{BS}^2 - \left(\frac{P_{BS}^2}{C_{SI}^2}\right) > 0 \tag{13}$$

This is the condition for full duplex gain in uplink. Similar to (7), given channel characteristics and received noise power at the BS, this condition is a function of UE2 and BS transmit powers (i.e., P_{UE} and P_{BS}), self-interference cancellation gain (C_{SI}), and the distance between BS and UE2 (d_2). Given locations of UEs, this condition combined with the downlink condition in (7) can be used to determine the transmit powers, P_{UE}, and P_{BS} , so that full duplex gain can be achieved in both downlink and uplink. In addition, given UE locations and transmit powers, this condition can also be used to derive the minimum required BS self-interference cancellation such that the uplink full duplex operation has throughput gain compared to the half duplex baseline. In fact, from (13), one can find

$$C_{SI} > P_{BS} \left(\frac{P_{UE} N_{BS}}{C_2 d_2^{\alpha_2}} + N_{BS}^2\right)^{-1/2} \tag{14}$$

Figure 5 shows the minimum required C_{SI} for LOS and NLOS channels between the UE and BS. Once again the results show that favorable propagation between the base station and UEs improve the performance of the full duplex system, here in terms of reducing the degree of BS self-interference cancellation required.

IV. Scheduling

The previous sections show that full duplex throughput gain is only available under certain propagation, range and power conditions. This observation indicates the need for an intelligent scheduler, which can use the full duplex capability opportunistically. That is, it must select the appropriate combination of UEs for full duplex operation in each timeslot,

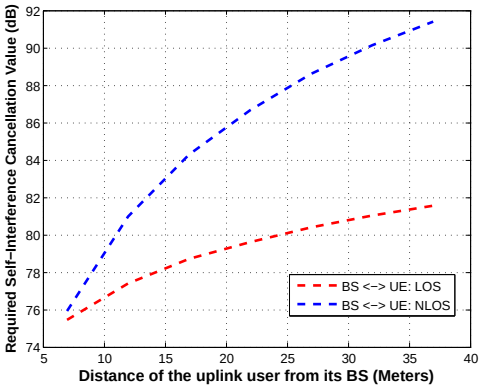

Fig. 5: Minimum required self-interference with different channel conditions (P_{BS} = 1.78 dBm, and P_{UE} = 0.78 dBm).

attempt to maximize system throughput, and maintain a level of fairness so all UEs are provided with service. The scheduler we propose will identify favorable conditions for full duplex operation and operate with a combination of full duplex and half duplex timeslots. We use a utility based scheduling algorithm for both the the half duplex baseline and full duplex system. Moreover, in our system, we also assume that each UE has infinite backlogged data for each direction.

A. Scheduling in the half-duplex system

In a multiuser scenario, in each scheduling interval, the objective of the scheduler is defined to maximize the logarithmic sum of the average rates of all the UEs [18], that is,

$$Maximize \ \sum_{k=1}^{N} log(\overline{R_k}(t)), \tag{15}$$

where N is the number of UEs in the system, and $\overline{R_k}(t)$ is the average achieved rate of UE k until timeslot t. In each timeslot, the scheduler calculates the utility index of each UE, and chooses the UE with maximum utility index. For each UE ($1 \leq k \leq N$), the value of $\overline{R_k}(t)$ depends on the scheduling decision in timeslot t, and it is updated as,

$$\overline{R_k}(t) = \begin{cases} \beta \ \overline{R_k}(t-1) + (1-\beta) \ R_k(t) & \text{if } k \text{ is scheduled} \\ & \text{at timeslot } t, \\ \beta \ \overline{R_k}(t-1) & \text{otherwise.} \end{cases} \tag{16}$$

where β is a weight constant taking a value between 0 and 1, and $R_k(t)$ is the instantaneous rate of user k that can be achieved in timeslot t. Assume UE m is selected in timeslot t, then based on (16) the value of the objective function given in (15) becomes

$$\sum_{k=1}^{N} log(\overline{R_k}(t)) = log(\beta \ \overline{R_m}(t-1) + (1-\beta) \ R_m(t)) - log(\beta \ \overline{R_m}(t-1)) + \sum_{k=1}^{N} log(\beta \ \overline{R_k}(t-1)), \tag{17}$$

which can be further reduced to,

$$\sum_{k=1}^{N} log(\overline{R_k}(t)) = log(\beta \ \overline{R_m}(t-1) + (1-\beta) \ R_m(t)) - log(\overline{R_m}(t-1)) + C. \tag{18}$$

where C is a constant and does not depend on the UE selection in timeslot t. It means that to maximize the objective function in timeslot t, the scheduler needs to choose a UE k as

$$\arg\max_{1\leq k\leq N} \; [log(\beta\ \overline{R_k}(t-1)+(1-\beta)\ R_k(t))-log(\overline{R_k}(t-1))]. \tag{19}$$

In each timeslot the scheduler calculates the above utility index of all UEs, and selects the one with the maximum value. In the half duplex system, where we assume that the downlink UEs and the uplink UEs are scheduled in alternative timeslots, the scheduling is done independently. That is, the scheduler maintains the average downlink throughput status (say $\overline{D_k}(t)$) and average uplink throughput status (say $\overline{U_k}(t)$) for each UE, separately. Then in each timeslot, the scheduler calculates the utility index for each UE in the corresponding direction and chooses the UE with the maximum index. For example, if t is a downlink timeslot, then the scheduler chooses a UE as

$$\arg\max_{1\leq k\leq N} \; [log(\beta\ \overline{D_k}(t-1)+(1-\beta)\ D_k(t))-log(\overline{D_k}(t-1))], \tag{20}$$

where $D_k(t)$ is the instantaneous downlink rate of UE k in time slot t. Once the UE selection is done, the average rate $\overline{D_k}(t)$ for all users ($1 \leq k \leq N$) is updated as described in (16). Please note that the average downlink rate for all users do not change during the uplink timeslot. A similar calculation is done for an uplink time slot with the uplink data rates.

B. Scheduling in the full duplex system

In the case of full duplex operation, where both the uplink and downlink UEs may be scheduled simultaneously, the scheduler needs to choose an appropriate UE in both directions. The objective of the scheduler is now defined as,

$$Maximize \;\; \sum_{k=1}^{N} log(\overline{D_k}(t)) + \sum_{k=1}^{N} log(\overline{U_k}(t)), \tag{21}$$

In each timeslot, the full duplex scheduler needs to calculate the utility indices for both directions. As we saw in Section II each direction degrades the performance of other direction by generating interference, so UE selection in one direction affects the selection in the other direction. Thus, in each timeslot, for the given self-interference cancellation capability, transmission powers, and the collection of UEs, a full duplex scheduler selects a pair of UEs with the maximum aggregate utility index (Agg_{ut}). It calculates the aggregate utility index for each pair and selects the one with the maximum value, that is,

$$\begin{aligned}\arg\max_{\substack{1\leq k,m\leq N\\ m\neq k}} \; & [\, log(\beta\ \overline{U_k}(t-1)+(1-\beta)\ U_k(t))-log(\overline{U_k}(t-1)) \\ & + log(\beta\ \overline{D_m}(t-1) + (1-\beta)\ D_m(t)) - log(\overline{D_m}(t-1))].\end{aligned} \tag{22}$$

The scheduler keeps track of the average rates (uplink/downlink) of each UE, and includes inter-UE interference and BS self-interference while calculating the instantaneous rates in each direction. In this way the full duplex scheduler tries to find the best pair for the given current condition while maintaining fairness and maximizing the overall objective (21).

In Section III, we derived the favorable conditions for full duplex operation from both the downlink and uplink UEs point of view. It was clear that sometimes a single UE in the uplink or downlink would be a better choice than full duplex operation. To implement this hybrid scheduling, our full duplex scheduler also calculates the independent downlink and the uplink utility index in each timeslot. It finds a downlink UE with the maximum downlink utility index (Dwn_{ut}), assuming no uplink UE on that channel, and also finds an uplink UE with the maximum uplink utility index (Up_{ut}) with no residual self-interference. Finally it selects one of the three cases with the maximum utility indices, that is

$$\max \;\; (Agg_{ut}, Dwn_{ut}, Up_{ut}). \tag{23}$$

Thus, our full duplex scheduler switches between full duplex operation and half duplex operation based on the utility gain in each timeslot. In other words, it selects the mode which contributes the largest value towards the overall objective of the system in terms of throughput as well as fairness.

V. Performance Evaluation

In this section, we present a simulation analysis comparing full duplex and half duplex operations of a single small cell in terms of the throughput and the energy efficiency. We use the scheduling algorithms described in Section IV along with parameters proposed by 3GPP for evaluating enhancements to LTE, in particular the Remote Radio Head (RRH)/Hotzone cell [17].

We consider a single rectangular RRH/Hotzone cell with dimensions $50m \times 60m$ having a BS in the center with ten randomly distributed UEs. The channel bandwidth is 10 MHz for both the half duplex and the full duplex systems. In the half duplex system, this channel is allocated alternately to a downlink and to an uplink UE. In the full duplex system it is allocated to either a pair of UEs in both directions or a single UE in a direction based on the scheduling decision. All other simulation parameters are described in Table I, based on 3GPP simulation recommendations for an RRH cell environment [17]. Path loss for both LOS and NLOS are given in Table I, where the probability of LOS (P_{LOS}) is,

$$P_{LOS} = \begin{cases} 1 & R \leq 0.018, \\ \exp\left(-(R-0.018)/0.027\right) & 0.018 < R < 0.037, \\ 0.5 & R \geq 0.037, \end{cases} \tag{24}$$

and R is the distance in kilometers. For a given UE at a distance R from the BS, a uniformly distributed random variable is generated, and compared with the P_{LOS} value. If it is less than or equal to P_{LOS} then LOS is chosen otherwise NLOS. A shadowing model is also considered for each channel. The channel model between BS and UE is used between mobile UEs for the full duplex interference calculations, with the expectation that in a small cell, BS and UE are comparable. This assumption would tend to provide

TABLE I: Simulation Parameters

Parameter	Value
Bandwidth	10 MHz
Number of Channels	1
Maximum BS Power	24 dBm
Maximum UE Power	23 dBm
Thermal Noise Density	-174 dBm/Hz
Noise Figure	BS: 8 dB, UE: 9 dB
Shadowing Standard Deviation (with no correlation)	LOS: 3 dB NLOS: 4 dB
Path Loss (dB) (R in kilometers)	LOS: $89.5 + 16.9\ log_{10}(R)$, NLOS: $147.4 + 43.3\ log_{10}(R)$

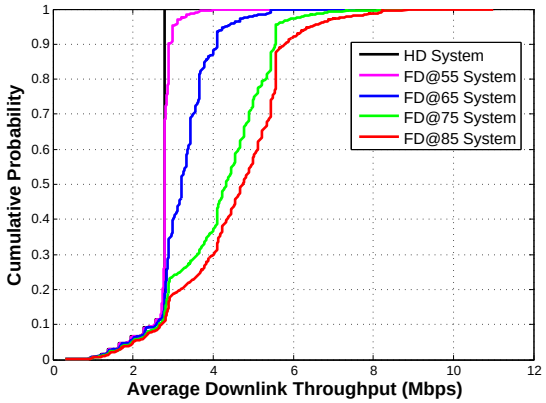

Fig. 6: Distribution of average data rates in downlink.

more conservation results for the full duplex system since one could argue that the typical UE-to-UE interference channel is likely to be poorer (therefore less UE-to-UE interference) than the typical BS-to-UE channel.

We assume a fixed power for each transmission in both downlink and uplink. This value is calculated by assuming a minimum performance requirement at the edge of the cell. In Section III we used the Shannon equation to derive favorable conditions for full duplex operation, but here we take a more pragmatic approach and use the LTE CQI table [19], [20]. The data rate for a given SNR/SINR is calculated as

$$DataRate = W_c E(1 - BLER), \tag{25}$$

where, for a given SNR/SINR, E is the spectral efficiency and BLER is block error rate of the corresponding CQI class. For our simulations, we put SNR requirement of $10.37dB$ (CQI Class 10) at the edge to calculate the required transmission power in both directions. Assuming NLOS propagation, the result is BS power (P_{BS}) of $1.78dBm$ and the UE power (P_{UE}) of $0.78dBm$. With this power settings, we run our simulation for different UE drops, each with a long time period, and generate results for both the half and full duplex systems.

Figures 6 and 7 show the distribution of average downlink and uplink rates over 500 random drops. Results for half duplex operation and full duplex operation with BS self-interference cancellation capability ranging from 55 to 85 dB ($FD@x$ means the full duplex system with self-interference cancellation of x dB) are drawn. The full duplex system

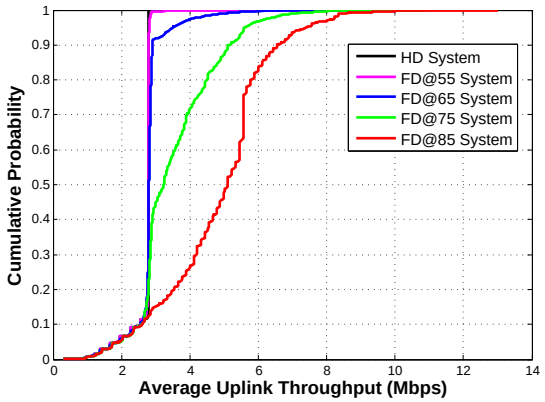

Fig. 7: Distribution average data rates in uplink.

TABLE II: Average performance gain of full duplex system over half duplex system.

	FD@55	FD@65	FD@75	FD@85
Downlink	2.0%	21%	56%	69%
Uplink	0.4%	4.9%	33%	81%

assigns full duplex, uplink or downlink slots based on the maximum index shown in (23).

As the self-interference cancellation capability increases, both the total average uplink and downlink throughput improves. Table II shows the average gain of the full duplex system compared to the half duplex system. With lower cancellation capability (e.g. 55 dB), the full duplex scheduler mostly defaults to half duplex operation (i.e., only one UE in a timeslot). As the cancellation capability is improved, the full duplex scheduler finds more favorable conditions for two UEs in a single timeslot and significant gain is shown over half duplex operation. For example, with 85 dB cancellation capability, the full duplex system provides 69% improvement in the downlink and 81% improvement in the uplink. Table II also shows that for low cancellation capability, uplink gain is lower than the downlink gain. However, as we reach 85 dB of cancellation and the self interference at the BS becomes less of an issue, the uplink shows more improvement than the downlink. As discussed in Section I, 85 dB is an achievable and perhaps even conservative value for base station performance [7], [8], [10], [11].

Figure 8 shows further details of the full duplex scheduler's operation, in particular, the hybrid operation which switches between the half duplex and the full duplex scheduling. The simulation maintains statistics on UEs which are scheduled in full duplex and half duplex modes. Figure 8 plots the distribution of those UE distances for each type of timeslot assignment. For each self interference cancellation value there are two curves, one with a solid line for the UEs that are scheduled in the full duplex mode, and another with dotted line for UEs which are scheduled in the half duplex mode. It is clear that UEs which are scheduled in full duplex timeslots are typically closer to the BS than the UEs which are scheduled in the half duplex timeslots. Moreover, the lower the BS self-interference cancellation capability, the closer the UEs to the

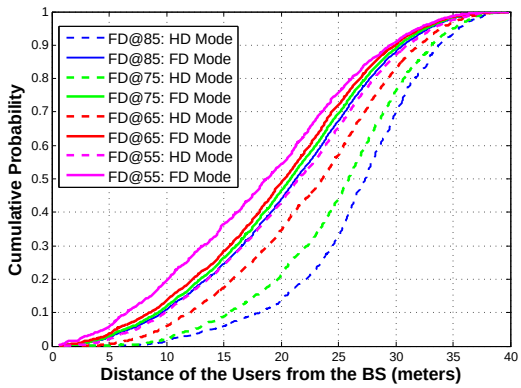

Fig. 8: Distribution of the UE distances scheduled in full duplex and half duplex modes.

TABLE III: Average energy efficiency in Gb/joule.

	HD	**FD@55**	**FD@65**	**FD@75**	**FD@85**
Downlink	35.5	35.2	34.4	32.8	32.3
Uplink	44.7	40.3	32.2	33.6	42.4

BS in the full duplex timeslots.

We also analyzed the energy efficiency by measuring a $bits/joule$ parameter. As described above we used the same fixed power per transmission in both directions. Thus, if a UE gets more timeslots to transmit due to the full duplex operation, it uses more power but also transmits more data.

Table III shows the average $bits/joule$ for each system in the downlink and uplink directions. In the downlink direction there is a small penalty in energy efficiency for full duplex operation, meaning that the additional transmit power is not completely offset by improved throughput. This additional power is consumed to overcome the interference from the simultaneous uplink transmission. Similarly, in the uplink direction, the additional power is used to compensate the residual self-interference during the full duplex operation. But in the uplink direction, the energy efficiency starts increasing again for higher self interference cancellation because of the lower residual self interference to compensate.

VI. Conclusion

In this work, we extend the application of common carrier full duplex radios to resource managed TDMA-type small cell systems. We derived the favorable conditions for increasing throughput due to full duplex operation compared to half duplex in a single cell scenario. We proposed a hybrid scheduler that switches between full duplex and half duplex modes based on the best available condition. Our simulation results show that a full duplex radio using currently available practical design parameters (i.e., 85 dB self interference cancellation) can improve the capacity compared to half duplex systems by 69% in the downlink and 81% in the uplink with a small penalty in energy efficiency. The reduced performance from the ideal doubling of capacity is due to interference issues particular to full duplex operation. As an extension of this work, we are analyzing the performance of full duplex radios in a multi-cell scenario and considering power control and MCS selection for such a system. We are also evaluating the performance of such system in more real mobile environment with fading and different available antenna models with sectored cells.

References

[1] Federal Communications Commission, "Mobile broadband: The benefits of additional spectrum," October 2010. [Online]. Available: www.fcc.gov

[2] Cisco, "Cisco visual networking index: Forecast and methodology 2012-2017," May 2013. [Online]. Available: www.cisco.com

[3] Ericsson, "Ericsson mobility report," June 2013. [Online]. Available: www.ericsson.com

[4] R. A. DiFazio and P. J. Pietraski, "The bandwidth crunch: Can wireless technology meet the skyrocketing demand for mobile data?" in *IEEE Long Island Systems, Applications and Technology Conference (LISAT)*, 2011, pp. 1–6.

[5] E. Business, "Searching for 1000 times the capacity of 4g wireless," July 2012. [Online]. Available: www.ebmag.com/Industry-News/searching-for-1000-times-the-capacity-of-4g-wireless.html

[6] Qualcomm, "The 1000x mobile data challenge," 2012. [Online]. Available: www.qualcomm.com/1000x

[7] J. I. Choi, M. Jain, K. Srinivasan, P. Levis, and S. Katti, "Achieving single channel, full duplex wireless communication," in *Proceedings of the sixteenth annual international conference on Mobile computing and networking (Mobicom)*, 2010, pp. 1–12.

[8] M. Knox, "Single antenna full duplex communications using a common carrier," in *IEEE 13th Annual Wireless and Microwave Technology Conference (WAMICON)*, April 2012, pp. 1 –6.

[9] D. Bharadia, E. McMilin, and S. Katti, "Full duplex radios," in *Proc. ACM SIGCOMM 2013*, 2013.

[10] A. Sahai, G. Patel, and A. Sabharwal, "Pushing the limits of full-duplex: Design and real-time implementation," *arXiv preprint arXiv:1107.0607*, 2011.

[11] M. Duarte, A. Sabharwal, V. Aggarwal, R. Jana, K. Ramakrishnan, C. Rice, and N. Shankaranarayanan, "Design and characterization of a full-duplex multi-antenna system for WiFi networks," *arXiv preprint arXiv:1210.1639*, 2012.

[12] S. Goyal, P. Liu, O. Gurbuz, E. Erkip, and S. Panwar, "A distributed MAC protocol for full duplex radio," in *Forty Seventh Asilomar Conference on Signals, Systems and Computers (ASILOMAR)*, 2013.

[13] S. Goyal, P. Liu, S. Hua, and S. Panwar, "Analyzing a full-duplex cellular system," in *Proc. Conference on Information Sciences and Systems (CISS)*, 2013.

[14] S. Barghi, A. Khojastepour, K. Sundaresan, and S. Rangarajan, "Characterizing the throughput gain of single cell mimo wireless systems with full duplex radios," in *10th International Symposium on Modeling and Optimization in Mobile, Ad Hoc and Wireless Networks (WiOpt)*, 2012, pp. 68–74.

[15] E. Dahlman, S. Parkvall, and J. Skold, *4G: LTE/LTE-Advanced for Mobile Broadband: LTE/LTE-Advanced for Mobile Broadband*. Academic Press, 2011.

[16] 3GPP, "Technical specification group radio access network; evolved universal terrestrial radio access (e-utra); physical channels and modulation," 3rd Generation Partnership Project (3GPP), TS 36.211, June 2012.

[17] ——, "Technical specification group radio access network; evolved universal terrestrial radio access (e-utra); further advancements for e-utra physical layer aspects," 3rd Generation Partnership Project (3GPP), TR 36.814, March 2010.

[18] D. Tse and P. Viswanath, *Fundamentals of wireless communication*. Cambridge university press, 2005.

[19] 3GPP, "Technical specification group radio access network; evolved universal terrestrial radio access (e-utra); physical layer procedures," 3rd Generation Partnership Project (3GPP), TS 36.213, Feb. 2013.

[20] C. Mehlführer, M. Wrulich, J. C. Ikuno, D. Bosanska, and M. Rupp, "Simulating the long term evolution physical layer," in *Proc. of the 17th European Signal Processing Conference (EUSIPCO), Glasgow, Scotland*, vol. 27, 2009.